



Impact toughness of friction stir processed low carbon steel used in shipbuilding



D.M. Sekban^a, S.M. Aktarer^b, P. Xue^c, Z.Y. Ma^c, G. Purcek^{d,*}

^a Department of Naval Architecture and Marine Engineering, Karadeniz Technical University, Trabzon, Turkey

^b Department of Automotive Technology, Recep Tayyip Erdogan University, Rize, Turkey

^c Shenyang National Laboratory for Materials Science, Institute of Metal Research, Chinese Academy of Sciences, Shenyang, China

^d Department of Mechanical Engineering, Karadeniz Technical University, Trabzon, Turkey

ARTICLE INFO

Article history:

Received 29 May 2016

Received in revised form
22 June 2016

Accepted 22 June 2016

Available online 23 June 2016

Keywords:

Friction stir processing

Low carbon steels

Impact toughness

ABSTRACT

Effect of single-pass friction stir processing (FSP) on the impact toughness of a low carbon steel mainly used in shipbuilding was investigated via Charpy impact test at different temperatures, and the results were correlated with the radical microstructural alterations during processing. A fine-grained (FG) microstructure was achieved in the processed zone by both large deformation and simultaneous dynamic recrystallization of coarse-grained (CG) structure during FSP. The grain size of ferritic phase decreased from 25 μm down to about 3.0 μm after processing. This microstructural changes brought about a considerable increase in strength values of the steel with a slight decrease in its ductility values. More importantly, significant refinement in the FSPed steel increased the impact energies in the upper shelf and partially lower shelf energy regions, and it considerably decreased the ductile-to-brittle transition temperature (DBTT) from $-40\text{ }^\circ\text{C}$ for the CG steel to about $-65\text{ }^\circ\text{C}$ for the FG steel. The improvement in the impact toughness of the steel was attributed mainly to the substantial microstructural refinement with grains separated mostly by high-angle grain boundaries.

© 2016 Elsevier B.V. All rights reserved.

1. Introduction

Despite the usage of a great variety of materials like composites and aluminum alloys, various types of steels are still utilized for shipbuilding industry [1]. Among them, low carbon steels have extensively been used in that construction industry due to their high workability, excellent weldability and low cost. Among such kind of steels, the steel called Grade A is one of the most widely used ones [2]. However, it is well known that they have relatively high ductile-to-brittle transition temperature (DBTT), which may have a problem in applications where the extreme environmental conditions are operated. Depending on dropping in temperature, almost all structural steels used for ship construction can undergo cleavage or tearing fracture mode [3]. Cleavage fracture occurs with a radical temperature decrease or increase in loading rate.

It is well known that low temperature fracture caused many tragedies for man-made steel structures in last two centuries [4]. For instance, Royal Mail Ship Titanic sank due to the freezing sea temperature at which steel hull plate of the ship became brittle and this ended up with its sinking [5]. Also, during the World War

2, over 4000 ships in various sizes were built, and more than 25% of them experienced a serious or potentially serious brittle fracture by the end of war [6]. Some of these fractures were catastrophic failures with breaking of the ships completely into two parts [7]. Therefore, the impact toughness and ductile-to-brittle transition temperature of such kind of steels used especially in ship building has become one of the most important features in applications where the steel parts are used in low temperatures.

In order to decrease the fracture risk or improve the toughness of steels, one of the measures is to improve the DBTT of steels by any means. Considering the marine applications, limited studies have been undertaken especially on improving the impact toughness of Grade A low carbon steel. Depending on the available literature, only one study was published about enhancing of mechanical and fracture properties of Grade A steel [1]. In that study, mechanical properties of quenched Grade A steel were investigated. It was found that while its hardness and strength increased, impact toughness decreased after quenching at room temperature. But, no study has been undertaken on improving the DBTT of low carbon shipbuilding steels.

Shipbuilding industry, on the other hand, generally uses thicker plates where high impact toughness and high strength are needed. This also results in increasing the total mass of the ship which

* Corresponding author.

E-mail address: purcek@ktu.edu.tr (G. Purcek).

brings about relatively high fuel conception and more releasing of CO₂ to the environment. Therefore, mechanical and fracture properties of the steels used in shipbuilding should be improved simultaneously. For fulfilling the property requirements, grain refinement down to micron or submicron sizes seems to be a viable way for improving both strength and toughness as well as decreasing ductile-to-brittle transition temperature of steels [8–12].

Friction stir processing (FSP) seems to be one of the most reliable methods for grain refinement of large scale plate or sheet type materials [13]. This is a novel microstructural modification method based on the basic principles of friction stir welding (FSW) [14,15]. In that process, a non-consumable rotating tool with a shoulder and pin insert into a metal plate or sheet and traverses through a direction of interest. The heat generated by friction between rotating tool and metal surface locally softens the volume to be processed. Material flowing around the pin and the tool shoulder undergoes severe plastic deformation and thermal exposure by traversing the rotating tool. The processed zone is constituted generally by recrystallized fine grains, fragmented primary particles and uniformly distributed second phase particles. In many cases, FSP leads to the transformation of the coarse-grained (CG) initial microstructure into equiaxed fine-grained (FG) and/or ultrafine-grained (UFG) structures consisting mostly of high angle grain boundaries (HAGBs) [16–19]. Many reports have been published on this process so far, and thus more detailed information on its principles can be obtained in [14,15,20,21].

In view of the above, the purpose of the present study is to improve fracture properties of Grade A shipbuilding steel by FSP. Also, alteration of its ductile-to-brittle transition temperature by FSP was also investigated to evaluate the temperature-induced change in the fracture mode.

2. Experimental procedure

Hot rolled low carbon steel plates known as Grade A with the chemical composition of 0.16 wt% C, 0.18 wt% Si, 0.7 wt% Mn, 0.11 wt% S, 0.18 wt% P, 0.09 wt% Cr, 0.14 wt% Mo, 0.04 wt% Cu, 0.04 wt% V and balance Fe was used in the current study. Samples with the dimensions of 200 mm × 40 mm × 6 mm were cut from the steel plates before FSP. FSP was performed with a WC tool

having a convex shoulder with the diameter of 18 mm and a conical pin with the diameter, length and cone angle of 8 mm, 3.5 mm and 15°, respectively. FSP was conducted with a tool rotation of 635 rpm and a traverse speed of 45 mm/min. The shoulder tilt angle was set at 3°, and the tool plunger downforce was kept constant at 11 kN during the process. Two schematic pictures representing the applied FSP, main processing parameters, the shape and location of the specimens inside the FSPed plate and also its cross sectional view showing the depth and the shape of the processed region are shown in Fig. 1(a)–(b). It is seen that a processed region with a depth of about 3.8 mm and a width close to the diameter of the tool shoulder (18 mm) form during FSP.

Optical microscope (OM) and transmission electron microscope (TEM) were used to observe the microstructure of the samples before and after FSP. The specimens for OM were cross-sectioned on the processed sample perpendicular to the processing direction (Fig. 1(a)), polished with standard techniques and then etched in 3% Nital (3 ml HNO₃ + 97 ml C₂H₆O) solution for 15 s. The TEM was performed using an FEI Tecnai F20 microscope, operated at a nominal voltage of 200 kV.

Mechanical properties of the samples before and after FSP were determined with tensile test using dog-bone shaped specimens with the dimensions of 2 mm × 3 mm × 26 mm. The tensile specimens were cross-sectioned parallel to the process direction (Fig. 1(a)). The tests were performed using an Instron-3382 electro-mechanical load frame with a video type extensometer at a strain rate of $5.4 \times 10^{-4} \text{ s}^{-1}$.

The impact toughness of steel plates was evaluated by measuring the total absorbed energy using Charpy impact test prior and after FSP. Subsize Charpy V-notched samples were cut from the CG and FG plates according to the German standard of DIN50115. The samples with the dimensions of 3 mm × 4 mm × 27 mm with a V-notch depth of 1 mm and a radius of 0.1 mm were machined from the processed zone of the FSPed plates perpendicular to the process direction (Fig. 1(a)). The impact tests were done within the temperature ranging between –180 °C and 20 °C. The test temperature was controlled by a pre-established calibration function based on thermocouple measurements. The fracture surfaces of the specimens were also observed using a JEOL 6400 SEM operated at 15 keV in the secondary

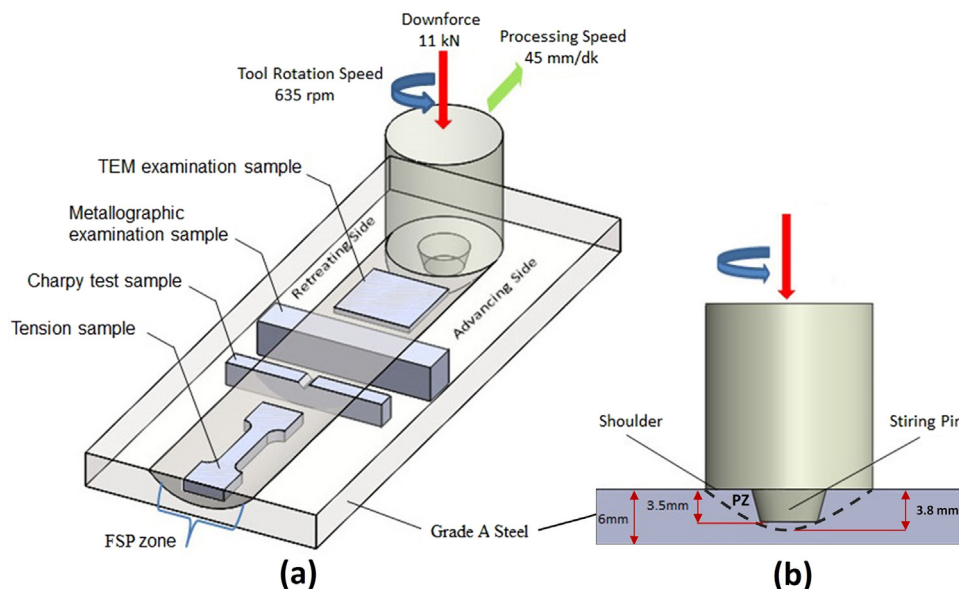


Fig. 1. (a) Schematic illustrations of the FSPed plate and the sample geometries machined from that plate. (b) Cross-sectional view of the plate showing the WC tool's position with the geometrical parameters.

electron imaging mode.

3. Results

3.1. Microstructure and mechanical properties

The initial microstructure of steel plate consists of CG ferrites with an average grain size of $25\ \mu\text{m}$ as well as smaller grains of

fine pearlite (Fig. 2(a)). Single-pass FSP resulted in a considerable refinement in the microstructure of the steel into the PZ (Fig. 2(b)–(e)). A FG microstructure formed with decreasing the grain size especially for the ferritic phase from $25\ \mu\text{m}$ to about $3.0\ \mu\text{m}$ in that zone (Fig. 2(b)). The coarse ferrite and pearlite grains were fragmented and refined by the simultaneous effects of both severe plastic deformation and dynamic recrystallization during FSP [22]. The microstructure of the PZ was characterized by the presence of ferrite and ferrite-pearlite boundaries and a ferrite/carbide

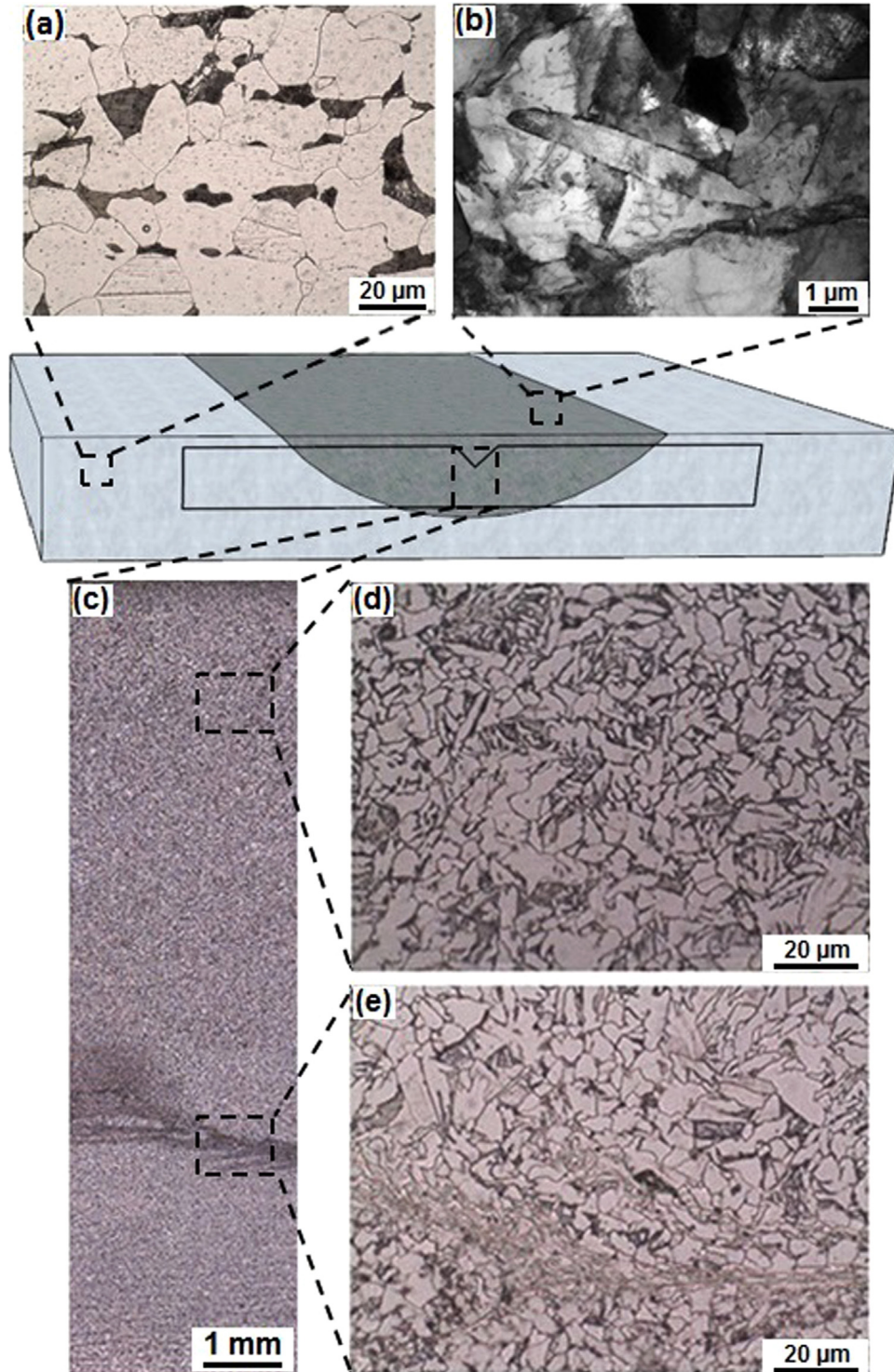


Fig. 2. (a) Optical micrograph showing the microstructure of un-processed coarse grained steel plate. (b) TEM micrograph showing the microstructure of FG FSPed region. (c)–(e) Optical micrographs showing the microstructures of FG FSPed low carbon steel plate along the vertical section.

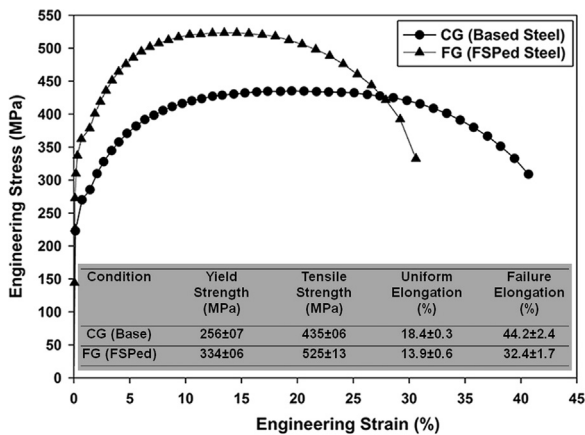


Fig. 3. Room temperature engineering stress-strain curves and main mechanical properties taken from these curves of the CG and FG steel plates.

aggregate that appears as fine pearlite [23].

It is apparent from the discrete fine grains in TEM micrograph that refined grains are separated mostly by high-angle grain boundaries. TEM micrographs also show that the FG microstructure includes dislocations (Fig. 2(b)). However, the dislocations in the microstructures are unevenly distributed in such a way that some grains in their central parts are rather free of dislocations, and most of the dislocations are accumulated and tangled with others around grain boundaries (Fig. 2(b)). Such distribution of the dislocations is normal. Because dynamic recovery and partly recrystallization occur during deformation, which spread the trapped lattice dislocations into grain boundaries [22].

The stress-strain curves of the steel before and after FSP and the main mechanical properties taken from these curves are shown in Fig. 3. As clearly seen, the steel before FSP exhibited low strength but good ductility due to its CG microstructure. Single-pass FSP increased considerably its strength without considerable decrease in ductility. Both yield and tensile strength values increased from 256 MPa and 435 MPa to 334 MPa and 525 MPa, respectively (see the table inside Fig. 3). The elongation to failure decreased slightly from 44% to about 32%. The uniform elongation also decreased slightly from 18% to about 14%.

The increase in strength values can be attributed to the grain refinement (Hall-Petch effect) and increase in dislocation density (strain hardening effect) by the effect of FSP [12]. The Hall-Petch effect is more pronounced on strengthening compared to that of strain hardening because of dynamic recrystallization during FSP. It is known that dislocation density also increases during FSP, and this formation makes a further effect on strengthening of the FSPed microstructure [24]. The formation of dislocations and their re-arrangement along the grain/subgrain boundaries during FSP are seen in Fig. 2(b). Such microstructural changes also brought about a slight decrease in ductility of that steel due to decreasing in strain hardening capability coming from an increase in dislocation density during FSP [25]. However, it should be noted that ductility values did not radically decrease after FSP compared to classical severe plastic deformation techniques. This can be attributed to the microstructure formed during FSP. As mentioned earlier, the grain size decreases both by severe plastic deformation and dynamic recrystallization during FSP [22]. Therefore, dislocation density does not increase radically during deformation by FSP in contrast to other cold severe plastic deformation techniques. A slight decrease in uniform elongation indicates the effects of grain refinement and also moderate increase in dislocation density.

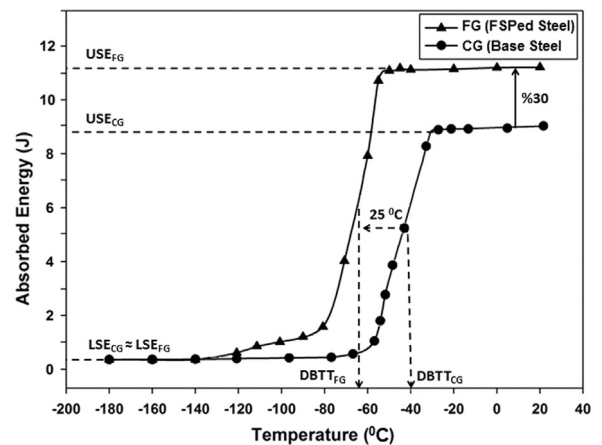


Fig. 4. Variation of Charpy absorbed energy as a function of test temperature in the range between -180 °C to 20 °C for both CG and FG steel samples.

3.2. Impact properties

3.2.1. Impact toughness and ductile to brittle transition temperature (DBTT)

Variation of Charpy absorbed energy as a function of temperature for both CG and FG steels are shown in Fig. 4. Selected toughness values taken from these curves are also summarized in Table 1. In general, the curves of both CG and FG steel samples exhibit a sharp drop (discontinuous change) in the absorbed energy in temperature range between the upper shelf energy (USE) and the lower shelf energy (LSE) regions. The curve of DBTT of CG steel shows a characteristic behavior for such steels [26–30]. The CG steel maintains the USE level down to about -30 °C, and then shows a narrow ductile-to-brittle transition range of about 20 °C. The DBTT is about -40 °C for the CG steel. The USE and the LSE of that steel are about 8.7 J and 0.2 J, respectively.

A reduction in the grain size down to micron level by FSP brought about a considerable change in the impact toughness behavior of the steel. The USE of the FG samples is higher than that of the CG samples. The USE increased from 8.7 J to about 11.2 J after grain refinement by FSP. This means that the impact toughness can be improved considerably with grain refinement even at room temperature by FSP. The USE of about 11 J was maintained from room temperature to about -55 °C for the FG steel. The LSE of steel was also enhanced after grain refinement depending on the temperature. At temperatures above -120 °C, the LSE of FG sample is higher than that of CG one. But below that temperature, the LSE of FG steel is approaching to that of CG one, and both CG and FG steel samples become almost the same energy level (Fig. 4). The DBTT of CG steel decreased after grain refinement by FSP. The DBTT decreased from -40 °C for the CG sample to about -65 °C for the FG sample. It is important to note that the LSE of FG steel exhibited a more gradual decrease in the absorbed energy especially in-between -80 °C to -120 °C.

3.2.2. Fracture characteristic

SEM fractographs of both CG and FG samples after impacting at room temperature are shown in Fig. 5. Both samples did not break completely during impacting at room temperature. The FG

Table 1
Impact toughness values of CG and FSPed FG low carbon steels.

| Condition | Grain size (μm) | USE (J) | LSE (J) | DBTT ($^{\circ}\text{C}$) |
|------------------|------------------------------|---------|---------|-----------------------------|
| CG (Base Steel) | 25 ± 3 | 8.7 | 0.2 | -40 |
| FG (FSPed Steel) | 3 ± 0.1 | 11.2 | 0.2 | -65 |

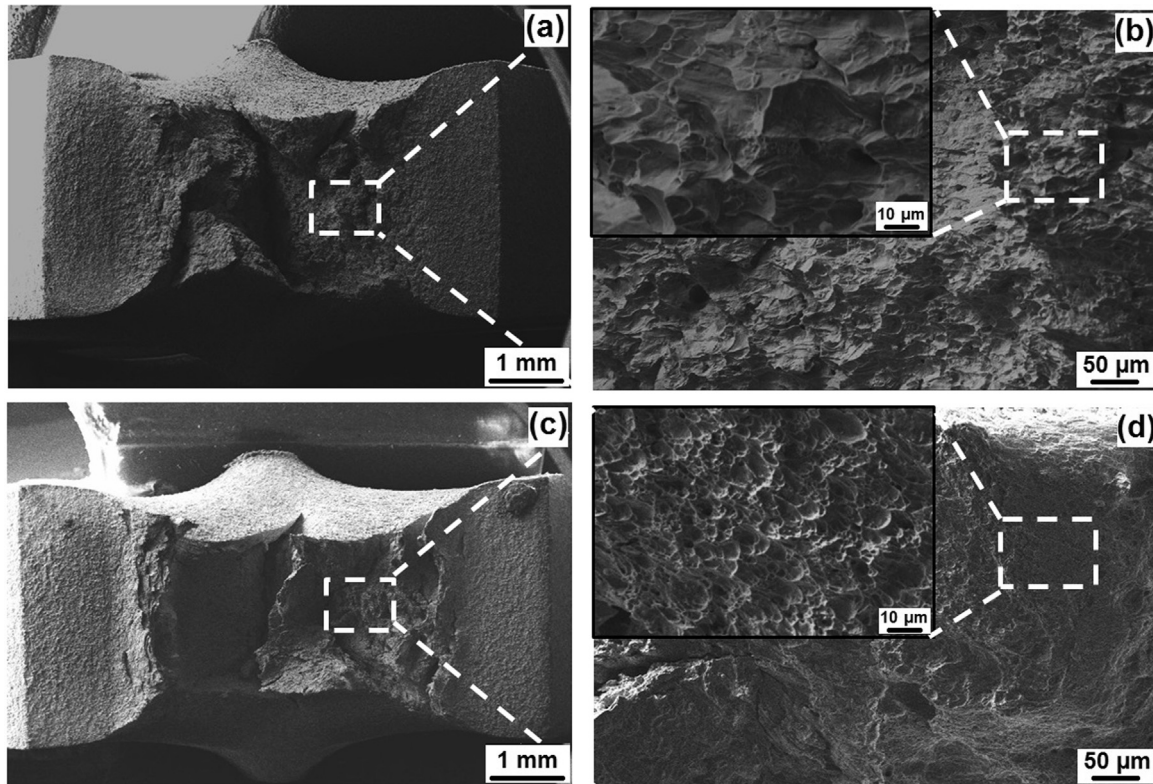


Fig. 5. SEM fractographs showing the fracture surfaces of the samples after impacting at room temperature: (a)–(b) CG sample and (c)–(d) FSPed FG sample.

sample after FSP exhibited almost the same fracture characteristic compared with the CG sample. The impacting caused tearing with large facets in the CG sample without separation (Fig. 5(b)). The fracture mode is ductile in both CG and FG samples, and the fracture takes place by the nucleation, growth and coalescence of microvoids (Fig. 5). While an appearance of fine dimple-like fracture surface is evident in the FG sample (Fig. 5(d)), quite coarser dimple-like fracture is seen in the CG sample (Fig. 5(b)). Because the CG sample exhibits large voids and hills due to its coarse-grained structure.

SEM fractographs of the CG samples after impacting at different temperatures from $-30\text{ }^{\circ}\text{C}$ to $-180\text{ }^{\circ}\text{C}$ are shown in Fig. 6. As seen, the samples do not break completely, and the micrograph of fracture surface showed coarse dimple-like fracture at the temperatures above $-50\text{ }^{\circ}\text{C}$ (Fig. 6(a)–(b)). At temperature of $-50\text{ }^{\circ}\text{C}$, the fracture changes from ductile to the brittle fracture mode. At that temperature and below it, fracture surfaces show purely brittle fracture mode, and cleavage facets with the sizes in range of $10\text{--}40\text{ }\mu\text{m}$ form throughout the fracture surface without any ductile tearing or dimple formation (Fig. 6(c)–(f)). This transition in fracture mechanism is in good agreement with the transition curve given in Fig. 4.

The fracture surface characteristics of FG samples after impacting at temperatures from $-60\text{ }^{\circ}\text{C}$ to $-180\text{ }^{\circ}\text{C}$ are shown in Fig. 7. The samples do not break completely above $-70\text{ }^{\circ}\text{C}$, and they exhibit an alligator in-type fracture mode (Fig. 7(a)). At or above the DBTT of $-60\text{ }^{\circ}\text{C}$, fracture surfaces consist of tearing zones with fine dimples indicating a dominant ductile fracture mode. At temperature of $-70\text{ }^{\circ}\text{C}$, the micrograph of fracture surface shows a transition situation, and the microstructure shows both ductile and brittle fracture modes at that temperature (Fig. 7(b)), which shows that the DBTT is around that temperature. Just below this temperature, fracture surface changes to the brittle fracture mode dominantly (Fig. 7(c)–(f)) as in the case of CG samples.

4. Discussion

Microstructural modification and grain refinement of low carbon steel by a single-pass FSP brought about considerable changes in its impact behavior and energy absorption depending on the temperature of impact test. The absorbed energy of the steel increased notably even at room temperature and through the USE region. This considerable improvement in the USE is attributed to the unique microstructure formed by FSP. As explained above, a FG microstructure with an average grain size of $3\text{ }\mu\text{m}$ was achieved with the grains separated mostly by high-angle of misorientation (Fig. 2). Because different grain refinement mechanism is operated during FSP in contrast to other SPD techniques. The microstructure changes radically by the intense and localized plastic deformation during FSP [9]. The tool and shoulder mix the material into the stir zone without changing the phases and create a modified microstructure having fine and mostly equiaxed grains separated mostly by HAGBs (Fig. 2). All of these changes brought about high strength and adequate ductility along with high toughness in FSPed steel [16–19]. It should be noted that most of previous studies reported a reduction in the USE of steels after grain refinement via conventional processing routes like rolling and forging. This was attributed to a radical decrease in ductility and the formation of anisotropic and multilayer (or elongated ferrite and accumulated second phase) structure formed by the effect of large plastic deformation [31–34]. Also low angle grain boundaries (LAGBs) along with HAGBs form during room temperature conventional and non-conventional plastic deformation processes. It is well known that the HAGBs are more effective in strengthening and also toughening of steels compared to the LAGBs [35]. Therefore, refined grains separated mostly by HAGBs effectively increase the absorbed energy even at room temperature by slowing the propagation of fracture. Furthermore, the current microstructure formed by FSP has no second phase formation, and also no multi-layered structure, which provide an additional

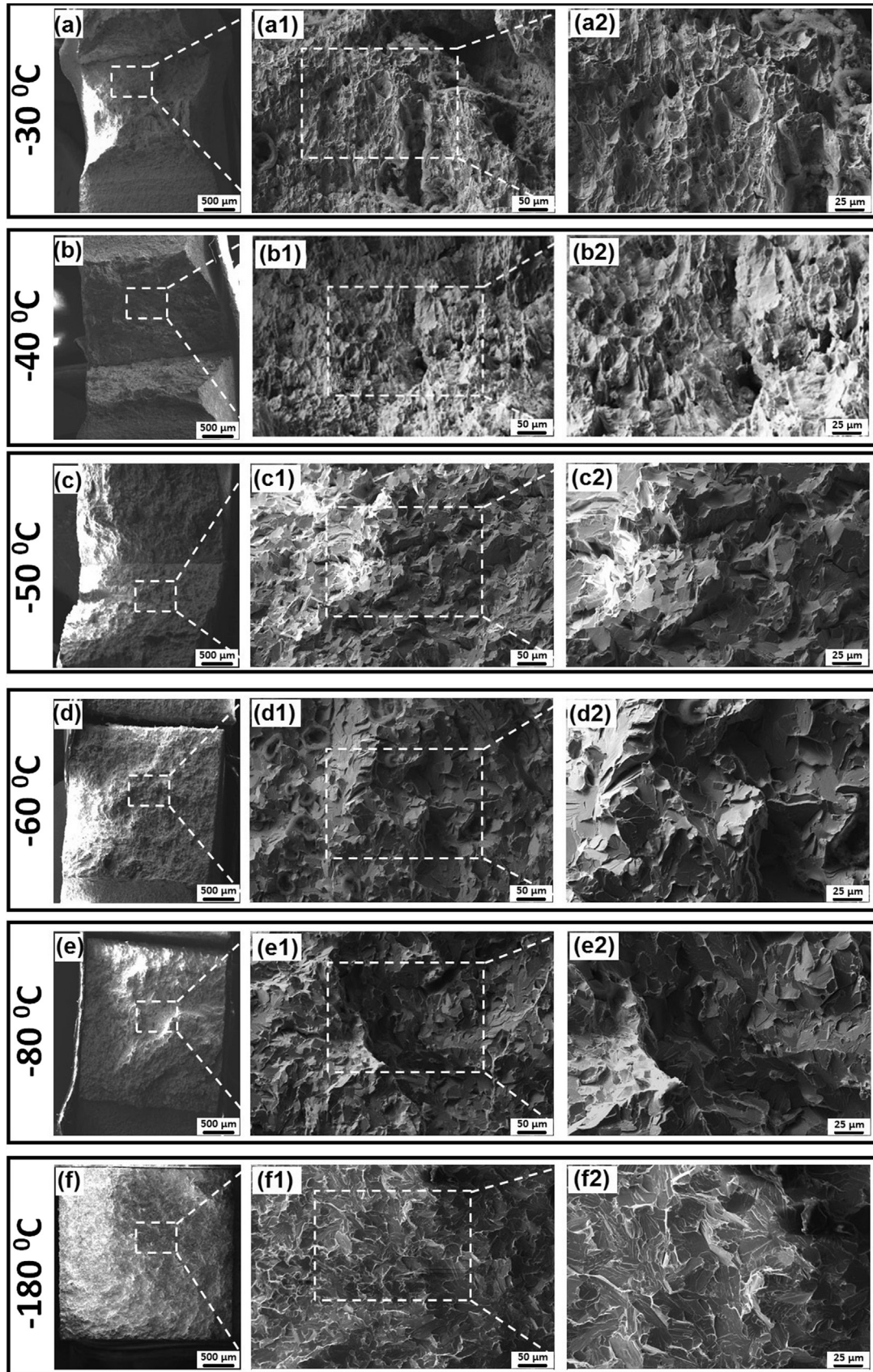


Fig. 6. SEM fractographs showing representative microstructures of the fracture surfaces of CG low carbon steel samples after impacting at different temperatures from -30 °C to -180 °C.

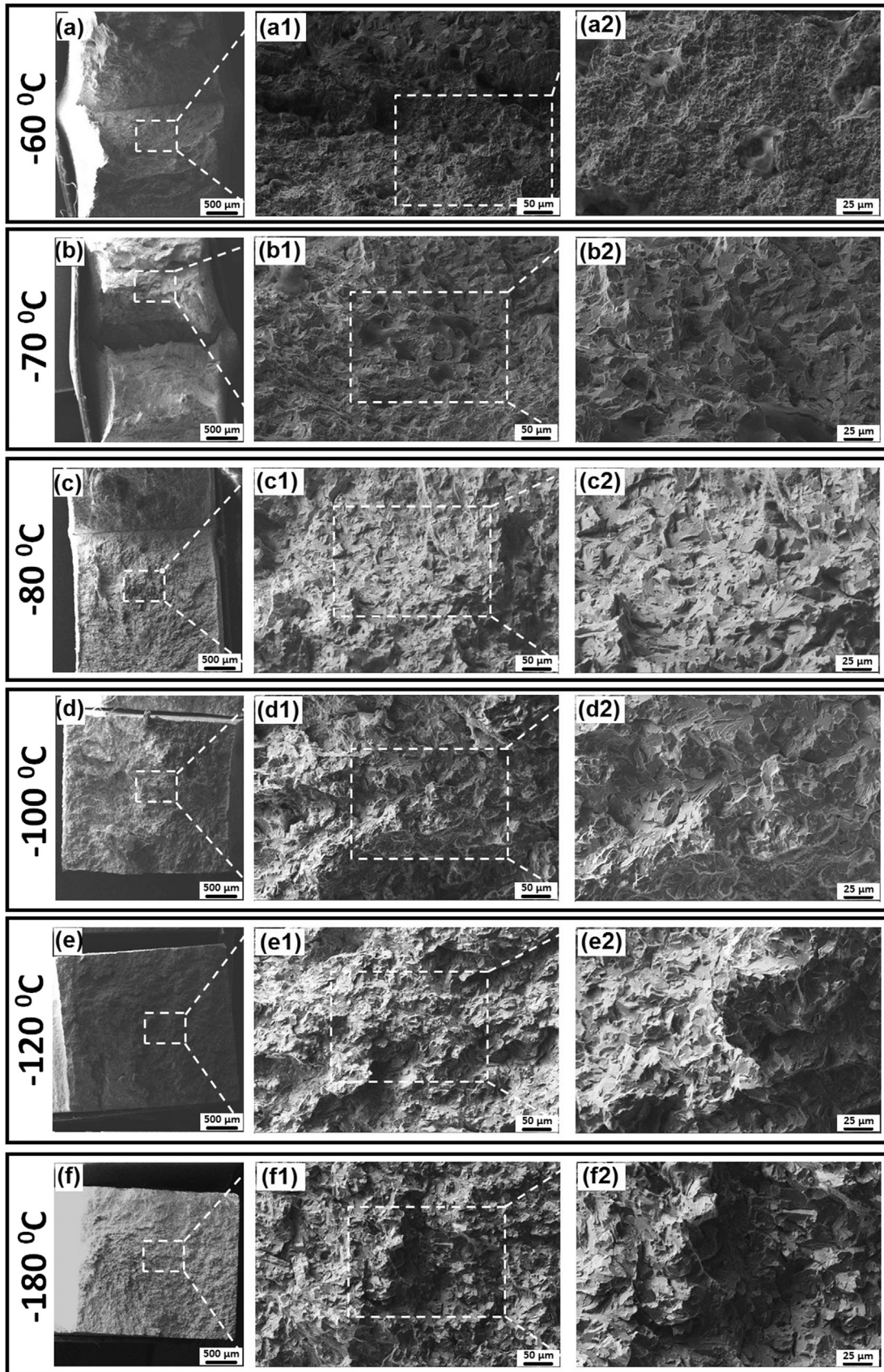


Fig. 7. SEM fractographs showing some representative microstructures for the fracture surfaces of FSPed FG samples after impacting at different temperatures from $-60\text{ }^{\circ}\text{C}$ to $-180\text{ }^{\circ}\text{C}$.

improvement in the toughness of USE region. However, some recent studies have reported that the USE of steels could be achieved by applying appropriate processing routes including some novel severe plastic deformation techniques [34]. But, it is important to note that the highest increase in the USE of steels was achieved in the present study among all published results.

The DBTT decreased from $-40\text{ }^{\circ}\text{C}$ for the CG steel to approximately $-65\text{ }^{\circ}\text{C}$ for the UFG steel. This improvement can also be explained by means of microstructural alteration during FSP. In bcc materials like steels, the DBTT is a result of the change in the fracture mechanisms from ductile to cleavage. At temperatures down to $-50\text{ }^{\circ}\text{C}$, ductile fracture mode with large deformation on the fractured surfaces was observed in the CG steel (Fig. 6). Below $-50\text{ }^{\circ}\text{C}$, the fracture mode changed from ductile to brittle accompanied by a sharp drop in the absorbed energy. Below that temperature, the fracture took place mostly by pure cleavage fracture mode (Fig. 6). Because, the resistance to the cleavage crack initiation and propagation is relatively low in the CG steel due to the large grains along the impacting area. The crack propagation in the CG steel cannot be blocked effectively by grain boundaries because of the large size of grains. It is known that the DBTT of many types of steels is affected mainly by the grain size and grain boundary misorientation [36]. Reducing grain size commonly results in a relatively low DBTT [33]. Decreasing grain size down to micron size affects the fracture mechanisms, and it slows down the initiation and propagation of cleavage cracking mode [33]. The grain refinement from $25\text{ }\mu\text{m}$ down to $3\text{ }\mu\text{m}$ by FSP significantly increased the amount of grain boundaries and brought about an improvement in the impact toughness as well as the DBTT (Fig. 4). More grain boundaries mean more barriers in front of the crack propagation during impacting. As the cleavage crack propagates along several grains, both the crack tip dislocations and the formation of cleavage facets are interrupted by these boundaries [31]. The crack paths are moved from one grain to another leaving micro-zigzag crack patterns, and more grain size in finer grains means more resistance to easy-crack propagation in the FG steel. Thus, decreasing grain size from CG to FG also decreases the propagation of initiated cleavage cracks and raises the fracture toughness in the transition region. On the other hand, it is also known that the HAGBs are more effective on this interruption compared to the LAGBs [37,38]. In the present study, the formation of fine grains separated mostly by HAGBs during FSP makes a further effect on decreasing the DBTT as in the case of improvement in the USE [39]. If the cleavage cracking moves across the HAGBs, then the crack front is branched together with the separation of the grain boundary between the grain breakthrough points, resulting in additional fracture work.

5. Conclusions

A low carbon steel used mainly for ship construction was processed by a single-pass FSP at room temperature to achieve a FG microstructure leading to a high strength-ductility-toughness balance. The main results and conclusions of this study can be summarized as follows:

1. A fine grained microstructure with an average grain size of $3\text{ }\mu\text{m}$ was achieved after processing of $25\text{ }\mu\text{m}$ grain size CG low carbon steel by FSP. This substantial grain refinement along with moderate dislocation accumulation brings about a significantly enhancement in strength values without notably sacrificing the elongation to failure and more importantly the uniform deformation behavior.
2. Microstructural modification by FSP causes a considerable alteration in the toughness behavior of low carbon steel. Grain

refinement by FSP enhances the toughness by increasing the USE and LSE and by decreasing the DBTT. The improvement in toughness at both high and low temperatures was attributed mainly to the substantial microstructural refinement and the refined grains separated mostly by high-angle grain boundaries (HAGBs).

3. The DBTT decreased from $-40\text{ }^{\circ}\text{C}$ for CG steel to $-65\text{ }^{\circ}\text{C}$ for FG steel after FSP as a result of a modified microstructure having micron sized grains separated mostly by HAGBs.
4. Cleavage-type fracture in CG steel is suppressed by the effect of grain refinement down to low temperatures. Ductile fracture mode becomes more effective down to the LSE region under impact loading after grain refinement by FSP.

Acknowledgments

Dr. G. Purcek was supported by “The World Academy of Sciences, Italy (TWAS)” under the Visiting Researchers Program of TWAS-UNESCO Associateship Scheme (Ref. 3240260896).

References

- [1] F. Hayat, H. Uzun, Effect of heat treatment on microstructure, mechanical properties and fracture behaviour of ship and dual phase steels, *J. Iron Steel Res. Int.* 18 (8) (2011) 65–72.
- [2] D.J. Eyres, *Ship Construction*, 5th Ed., Butterworth-Heinemann, Oxford, 2001.
- [3] J.D.G. Sumpter, A.J. Caudrey, Recommended fracture toughness for ship hull steel and weld, *Mar. Struct.* 8 (1995) 345–357.
- [4] V.V. Stoloyarov, R.Z. Valiev, Y.T. Zhu, Enhanced low-temperature impact toughness of nanostructured Ti, *Appl. Phys. Lett.* 88 (4) (2006).
- [5] K. Felkins, J.H.P. Leighly, A. Jankovic, The royal mail ship titanic: did a metallurgical failure cause a night to remember? *JOM-Us* 50 (1) (1998) 12–18.
- [6] H. Reemysynder, Ships that have broken in two pieces—World War II US maritime commission construction, Bethlehem Steel Internal Memo, 1402-1b, 1990.
- [7] J.D.G. Sumpter, J.S. Kent, Prediction of ship brittle fracture casualty rates by a probabilistic method, *Mar. Struct.* 17 (8) (2004) 575–589.
- [8] O. Saray, G. Purcek, I. Karaman, H.J. Maier, Impact toughness of ultrafine-grained interstitial-free steel, *Metall. Mater. Trans. A* 43A (11) (2012) 4320–4330.
- [9] D.M. Sekban, O. Saray, S.M. Aktarer, G. Purcek, Z.Y. Ma, Microstructure, mechanical properties and formability of friction stir processed interstitial-free steel, *Mater. Sci. Eng. A* 642 (2015) 57–64.
- [10] A. Chabok, K. Dehghani, M.A. Jazani, Comparing the fatigue and corrosion behavior of nanograin and coarse-grain IF steels, *Acta Metall. Sin. – Engl.* 28 (3) (2015) 295–301.
- [11] Y.C. Chen, K. Nakata, Evaluation of microstructure and mechanical properties in friction stir processed SKD61 tool steel, *Mater. Charact.* 60 (12) (2009) 1471–1475.
- [12] M. Hajian, A. Abdollah-zadeh, S.S. Rezaei-Nejad, H. Assadi, S.M.M. Hadavi, K. Chung, M. Shokouhimehr, Microstructure and mechanical properties of friction stir processed AISI 316L stainless steel, *Mater. Des.* 67 (2015) 82–94.
- [13] S.M. Aktarer, D.M. Sekban, O. Saray, T. Kucukomeroglu, Z.Y. Ma, G. Purcek, Effect of two-pass friction stir processing on the microstructure and mechanical properties of as-cast binary Al–12Si alloy, *Mater. Sci. Eng. A* 636 (2015) 311–319.
- [14] R.S. Mishra, Z.Y. Ma, Friction stir welding and processing, *Mater. Sci. Eng. R* 50 (1–2) (2005) 1–78.
- [15] Z.Y. Ma, Friction stir processing technology: a review, *Metall. Mater. Trans. A* 39A (3) (2008) 642–658.
- [16] S. Mironov, Y.S. Sato, H. Kokawa, Microstructural evolution during friction stir processing of pure iron, *Acta Mater.* 56 (11) (2008) 2602–2614.
- [17] C.G. Rhodes, M.W. Mahoney, W.H. Bingel, M. Calabrese, Fine-grain evolution in friction-stir processed 7050 aluminum, *Scr. Mater.* 48 (10) (2003) 1451–1455.
- [18] J.-Q. Su, T.W. Nelson, C.J. Sterling, Friction stir processing of large-area bulk UFG aluminum alloys, *Scr. Mater.* 52 (2) (2005) 135–140.
- [19] J.S. Pilchak, M.C. Juhas, J.C. Williams, Microstructural refinement and property enhancement of cast light alloys via friction stir processing, *Scr. Mater.* 58 (5) (2008) 361–366.
- [20] R.S. Mishra, P.S. De, N. Kumar, *Friction Stir Welding and Processing: Science and Engineering*, Springer, New York, 2014.
- [21] R.S. Mishra, Z.Y. Ma, I. Charit, Friction stir processing: a novel technique for fabrication of surface composite, *Mater. Sci. Eng. A* 341 (1–2) (2003) 307–310.
- [22] P. Xue, B.L. Xiao, W.G. Wang, Q. Zhang, D. Wang, Q.Z. Wang, Z.Y. Ma, Achieving ultrafine dual-phase structure with superior mechanical property in friction stir processed plain low carbon steel, *Mater. Sci. Eng. A* 575 (2013) 30–34.

- [23] B.T.J. Lienert, J.W.L. Stellwag, B.B. Grimmer, R.W. Warke, Friction stir welding studies on mild steel, *Weld. J. Res.* 82 (Suppl.) (2003) S1–S9.
- [24] J.Q. Su, T.W. Nelson, C.J. Sterling, Microstructure evolution during FSW/FSP of high strength aluminum alloys, *Mater. Sci. Eng. A* 405 (1–2) (2005) 277–286.
- [25] A. Chabok, K. Dehghani, Effect of processing parameters on the mechanical properties of interstitial free steel subjected to friction stir processing, *J. Mater. Eng. Perform.* 22 (5) (2013) 1324–1330.
- [26] Y.Y. Song, D.H. Ping, F.X. Yin, X.Y. Li, Y.Y. Li, Microstructural evolution and low temperature impact toughness of a Fe-13%Cr-4%Ni-Mo martensitic stainless steel, *Mater. Sci. Eng. A* 527 (3) (2010) 614–618.
- [27] B. Tanguy, J. Besson, R. Piques, A. Pineau, Ductile to brittle transition of an A508 steel characterized by Charpy impact test Part I: experimental results, *Eng. Fract. Mech.* 72 (1) (2005) 49–72.
- [28] Y.J. Chao, J.D. Ward, R.G. Sands, Charpy impact energy, fracture toughness and ductile-brittle transition temperature of dual-phase 590 steel, *Mater. Des.* 28 (2) (2007) 551–557.
- [29] M.C. Zhao, T. Hanamura, H. Qiu, F.X. Yin, H. Dong, K. Yang, K. Nagai, Low absorbed energy ductile dimple fracture in lower shelf region in an ultrafine grained ferrite/cementite steel, *Metall. Mater. Trans. A* 37A (9) (2006) 2897–2900.
- [30] R.O. Ritchie, W.L. Server, R.A. Wullaert, Critical fracture stress and fracture strain models for the prediction of lower and upper shelf toughness in nuclear pressure vessel steels, *Metall. Mater. Trans. A* 10 (10) (1979) 1557–1570.
- [31] R. Song, D. Ponge, D. Raabe, Mechanical properties of an ultrafine grained C-Mn steel processed by warm deformation and annealing, *Acta Mater.* 53 (18) (2005) 4881–4892.
- [32] T. Inoue, F.X. Yin, Y. Kimura, K. Tsuzaki, S. Ochiai, Delamination effect on impact properties of ultrafine-grained low-carbon steel processed by warm caliber rolling, *Metall. Mater. Trans. A* 41A (2) (2010) 341–355.
- [33] R. Song, D. Ponge, D. Raabe, J.G. Speer, D.K. Matlock, Overview of processing, microstructure and mechanical properties of ultrafine grained bcc steels, *Mater. Sci. Eng. A* 441 (1–2) (2006) 1–17.
- [34] K. Nagai, Ultrafine-grained ferrite steel with dispersed cementite particles, *J. Mater. Process. Tech.* 117 (3) (2001) 329–332.
- [35] M.C. Zhao, X.F. Huang, J.L. Li, T.Y. Zeng, Y.C. Zhao, A. Atrens, Strength and toughness tradeoffs for an ultrafine-grain size ferrite/cementite steel produced by warm-rolling and annealing, *Mater. Sci. Eng. A* 528 (28) (2011) 8157–8168.
- [36] B. Hwang, Y.G. Kim, S. Lee, Y.M. Kim, N.J. Kim, J.Y. Yoo, Effective grain size and charpy impact properties of high-toughness X70 pipeline steels, *Metall. Mater. Trans. A* 36A (8) (2005) 2107–2114.
- [37] S.Y. Shin, B. Hwang, S. Kim, S. Lee, Fracture toughness analysis in transition temperature region of API X70 pipeline steels, *Mater. Sci. Eng. A* 429 (1–2) (2006) 196–204.
- [38] S. Kim, Y.R. Im, S. Lee, H.C. Lee, Y.J. Oh, J.H. Hong, Effects of alloying elements on mechanical and fracture properties of base metals and simulated heat-affected zones of SA 508 steels, *Metall. Mater. Trans. A* 32 (4) (2001) 903–911.
- [39] R.O. Ritchie, J.F. Knott, J. Rice, On the relationship between critical tensile stress and fracture toughness in mild steel, *J. Mech. Phys. Solids* 21 (1973) 395–410.